Nano Biomed Eng
2018, 10(1): 46-55. doi: 10.5101/nbe.v10i1.p46-55.

Research Article

Preparation and Biological Activities of New Heterocyclic Azo Ligand and Some of Its Chelate Complexes

Siham Sami Al-Muhanaa, Abbas Hmood Al-Khafagy

Department of Chemistry, Faculty of Education for Women, University of Kufa, 54001 Najaf, Iraq.

Corresponding author. E-mail: sihamsami352@gmail.com

Received: Feb. 22, 2018; **Accepted:** Mar. 22, 2018; **Published:** Mar. 26, 2018.

Citation: Siham Sami Al-Muhanaa, Abbas Hmood Al-Khafagy, Preparation and Biological Activities of New Heterocyclic Azo Ligand and Some of Its Chelate Complexes. *Nano Biomed. Eng.*, 2018, 10(1): 46-55.
DOI: 10.5101/nbe.v10i1.p46-55.

Abstract

New azo ligand, 2[(Aminoantipyren) azo]-4,5-bis(4-Methoxyphenyl)-H imidazole, (AAMPI) was prepared through coupling reaction of 4-amino antipyrine with 4,5-bis (4-methoxyphenyl) imidazole. Then, complexation of ligand with ions Co(II), Ni(II), Cu(II), Zn(II), Cd(II) and Hg(II) were prepared to yield six complexes. The optimal conditions were studied for all complexes in the mole ratio between metal:ligand (M:L) as of 1:2 in the general formula $[M(L)_2]Cl_2 \cdot H_2O$. Present results found the azo ligand was tridentate. The structures of ligand with complexes were identified by ultraviolet-visible spectroscopy (UV-Vis), Fourier-transform infrared spectroscopy (FT-IR), proton nuclear magnetic resonance (^{1}HNMR), carbon-13 nuclear magnetic resonance (^{13}CNMR), mass spectrometry, elemental analysis (CHN), magnetic susceptibility and molar conductance. All the complexes exhibit octahedral geometry around the metal center. The antibacterial activities of synthesized compound were tested against the gram-negative, gram-positive bacteria and fungus. The results showed that the metal complexes exhibited antibacterial and antifungal activities compared with free ligand.

Keywords: Azo ligand; Imidazole; Metal complexes; Coupling reaction; Biological activity

Introduction

Azo dyes are known for extended applications in different fields and have been attracting the attention of synthetic and theoretical chemists [1]. Also, textile dyes, due to containing azo group -N=N- and the conjugated bonds, appear colored by the absorption of light in the visible region [2]. Azo compound derived from heterocyclic amines containing nitrogen in the aromatic rings and their metal complexes, particularly fused with imidazole or pyrazole as the heterocyclic, have been drawing the interest of many studies due to their biological activities [3, 4]. The imidazole ring is found in very significant endogenous biomolecules, such as biotin, the autacoid histamine and the essential amino acid histidine [5]. Additionally, the imidazole derivatives are highly important in medicinal chemistry research; a lot of imidazole-containing compounds show biological activities such as antifungal, antibacterial, anti-inflammatory and anthelmintic [6], antitubercular [7], antiblood pressures, antiallergic, antiasthma [8] and anticancer [9]. Antipyrine is well known for its pharmaceutical as well as medical applications including antibacterial, antifungal [10],

antituberculosis, anticancer [11], antitumor and antioxidant [12]. Depending on these results, we reported the preparation and characterization of the new heterocyclic azo dye ligand 2[(Aminoantipyren) azo]-4,5-bis(4-Methoxyphyl)-H imidazole (AAMPI) and its metal complexes for Co(II), Ni(II), Cu(II), Zn(II), Cd(II) and Hg(II) ions. The ligand and their metal complexes were screened for antibacterial activity against Klebsiella pneumoniae, Pseudomonas aeruginosa, *Prteus mirabillis*, *Staphylococus aureus* and *Stuphylococus epidermidis*, and were additionally screened for antifungal activity against *Aspergillus niger*, *Fusarium oxysparium* and *Trichoderma harzianum*.

Experimental

Materials and measurements

All chemicals were of highest purity and obtained from Fluka, Germany. Elemental analysis (C.H.N) was obtained using EA300 C.H.N elemental analyzer. Mass spectra were obtained using Agilent Technologies 5973C at 70 eV. The ^{1}HNMR and ^{13}CNMR spectrophotometry in DMSO-d6 was recorded on Bruker 500 MHZ spectrophotometer using tetramethylsilane (TMS) as an internal reference. The infrared (IR) spectra of azo ligand and its complexes were recorded in KBr in the range of 4000-400/cm on Fourier-transform infrared (FT-IR) test scan Shimadzu model 8400S. The ultraviolet-visible spectroscopy (UV-Vis) spectra were recorded in the range of 200-1100 nm in absolute ethanol on Shimadzu model 1650PC. Magnetic susceptibility measurements of the complexes were carried out on a magnetic susceptibility balance using faraday method; the diamagnetic corrections were made by Pascal's constants. Molar conductance measurements were recorded in ethanol by using 3IA Conductivity Bridge at room temperature. The metal contents of the complexes were measured by using atomic absorption technique by Shimadzu AA-160. Melting points were specified on SMP10 melting point.

Preparation of derivative imidazole

The imidazole derivative obtained from the reaction of benzyl derivative and hexamethylenetetramine in the presence of glacial acetic acid [13]. In a round flask (250 mL) was added 50 mL of glacial acetic acid to a mixture of benzyl derivative (2.90 gm, 0.01 mol), hexamethylenetetramine (0.256 gm, 0.005 mol) and ammonium acetate (6.0 gm, 0.23 mol). The solution reflux was heated for 90 min, by using reflected condenser. The solution was diluted after cooling by adding 400 mL of distal water. The imidazole derivative was precipitated by adding the solution of ammonium hydroxide. The white precipitate was collected by filtration, washed several times with distal water, re-crystallized from hot ethanol (to obtain white crystalline) and dried at room temperature. The yield was 79% and the m.p. was 72-74 °C.

Preparation of azo ligand (AAMPI)

According to the typical procedure [14], 30 mL of distilled water containing 3 mL of hydrochloric acid was added to 2.4 g of 0.01 mol 4-aminoantipyren, and cooled in ice bath. Then, a solution of 0.7 g 0.01 mol sodium nitrite in 10 mL of water was added dropwise. The formed Diazonium chloride was coupled with an alkaline solution of 2.80 g 0.01 mol 4,5-bis(4-Methoxy phenyl) imidazole, in 100 mL of ethanol. The orange solution was produced; the mixture was left in the refrigerator overnight. The precipitate was filtered off, washed several times in water and air-dried (Scheme 1).

Preparation of metal complexes

The metal complexes were prepared by dissolving 0.988 g of 0.002 mol ligand in 50 mL ethanol and added dropwise with stirring to 0.001 mol chlorides salts of Co(II), Cu(II), Ni(II), Zn(II), Cd(II) and Hg(II) dissolved in water [15]. The precipitated product was filtered and washed with water. Table 1 shows the physical properties and analytical data of the prepared azo ligand and its complexes.

Antimicrobial activity

All the newly synthesized compounds were evaluated for their in vitro antibacterial activity against several pathogenic gram-negative bacteria (*K. pneumoniae*, *P. aeruginosa* and *P. mirabillis*) and gram-positive bacteria (*S. aureus* and *S. epidermidis*). Well-diffusion method was used for determination of the preliminary antibacterial activity [16]. Wells of 6 mm in diameter were made in the ager plates by using sterile cork borer, and then the agar surfaces were inoculated with bacterium. The test compounds were dissolved in dimethyl form amide (DMF) to obtain a solution of 1000 ppm concentration. The wells were filled with 0.1 mL of the tested compounds by using a micropipette. All the plates were incubated at 37 °C for overnight. The inhibition zones formed after 24 h by the compounds against the particular bacterial strain were measured, and the antibacterial activity of

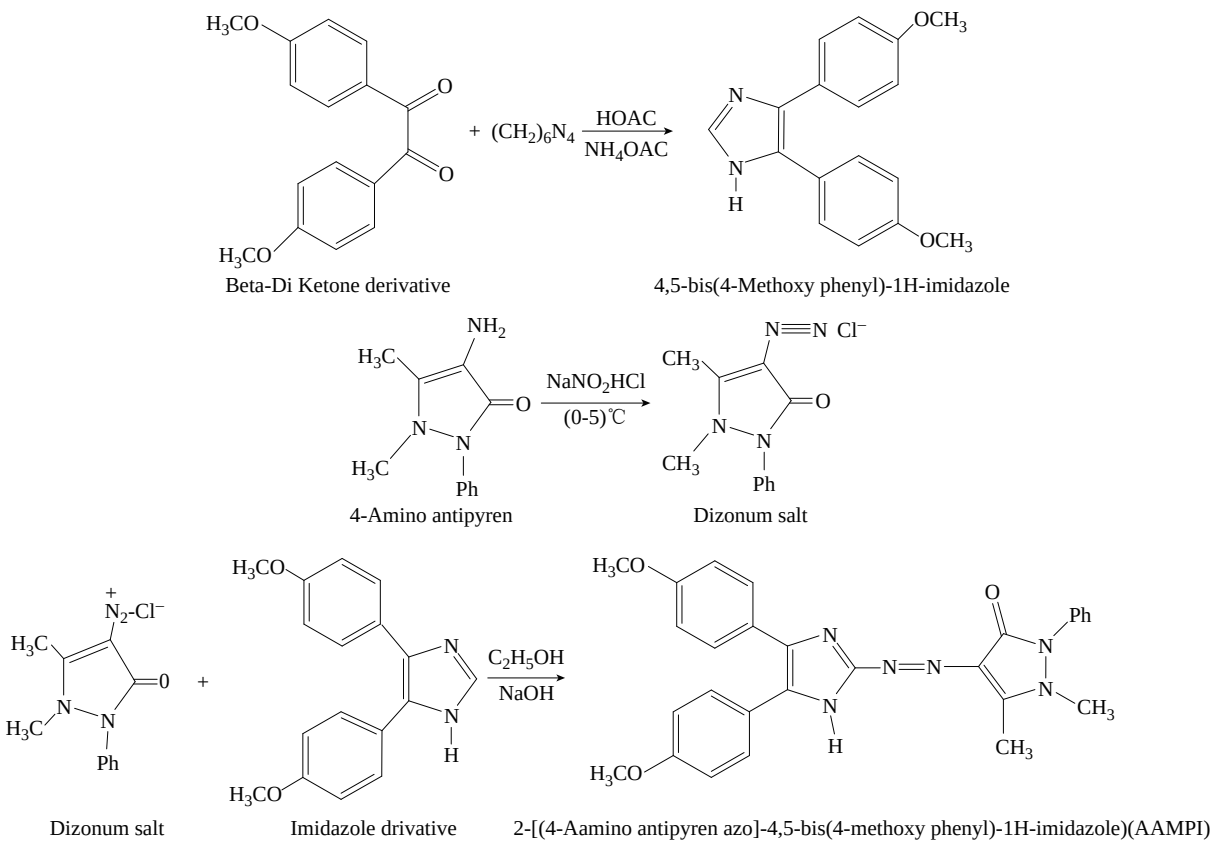

Scheme 1 Preparation of azo ligand (AAMPI).

Table 1 Elemental analysis and physical properties of ligand (AAMPI) and its metal complexes

No.	Cheimiecal formula	m.p (°C)	Color	Yield (%)	C% Found (cal.)	H% Found (cal.)	N% Found (cal.)	M% Found (cal.)
1	$(C_{28}H_{26}N_6O_3)$ =L	115-117	Orange	72	67.84 (68.01)	5.14 (5.26)	16.82 17.00	-
2	$[Co(L)_2]Cl_2{\cdot}H_2O$	198-200	Redish brown	86	58.98 (59.15)	4.64 (4.75)	14.66 (14.79)	4.97 (5.18)
3	$[Ni(L)_2]Cl_2{\cdot}H_2O$	193-195	Redish purple	80	58.92 (59.17)	4.62 (4.75)	14.64 (14.79)	4.94 (5.16)
4	$[Cu(L)_2]Cl_2{\cdot}H_2O$	140-142	Purple	81	58.71 (58.92)	4.64 (4.73)	14.59 (14.73)	5.32 (5.57)
5	$[Zn(L)_2]Cl_2{\cdot}H_2O$	238-240	Dark purple	78	58.55 (58.82)	4.61 (4.72)	14.57 (14.70)	5.72 (5.72)
6	$[Cd(L)_2]Cl_2{\cdot}H_2O$	136-138	Dark brown	69	56.36 (56.50)	4.41 (4.54)	13.93 (14.12)	9.33 (9.45)
7	$[Hg(L)_2]Cl_2{\cdot}H_2O$	150-152	Purple	83	52.45 (52.60)	4.12 (4.22)	12.97 (13.15)	15.65 (15.70)

the synthetic compounds was determined. The mean values were obtained for three individual replicates and were used to calculate the zone of growth inhibition for each compound.

The newly prepared compounds were also screened for their in vitro antifungal activity against *A. niger*, *F. oxysparium* and *T. harzianum* by well-diffusion method [17] at 250, 500 and 1000 ppm concentrations with triplicate determinations in each case. The average percentage inhibition was calculated using the following formula [18]:

Inhibition (%) = (C-T) 100/C,

where C is diameter of the colony fungus in center plates, and T is diameter of the colony fungus in the test plates.

Results and Discussion

The azo ligand and its metal complexes were soluble in methanol, ethanol, DMF, dimethyl

sulfoxide (DMSO) and acetone, but insoluble in water. Additionally, they were stable at room temperature. The analytical and physical properties of azo ligand and its metal complexes are explained in Table 1.

Mass spectra of new azo ligand

The mass spectra of the azo ligand (AAMPI) showed a mother base peak of ion at m/z = 494 which was attributed to the molecular weight of ligand (494 gm/mol), and the peak at (M^+) m/z^+= 280 was due to the molecular weight (280 g/mol) of ion derivative imidazole (Fig. 1).

^{1}HNMR spectra

The ^{1}HNMR spectra of the new azo ligand (AAMPI), was measured in TMS as an internal reference with DMSO as a solvent. The spectra of ligand showed a signal at 2.486 ppm due to the methyl group H_3C-C=C- of pyrazole molecule [19], a signal at 2.73 ppm due to the methoxy group [20] in derivative imidazole, a signal at 3.376 ppm due to the methyl group H_3C-N< of antipyrine ring, while a signal at 10.64 ppm due to the NH group in imidazole molecule, and a signal at 2.51 ppm due to the solvent proton (Fig 2).

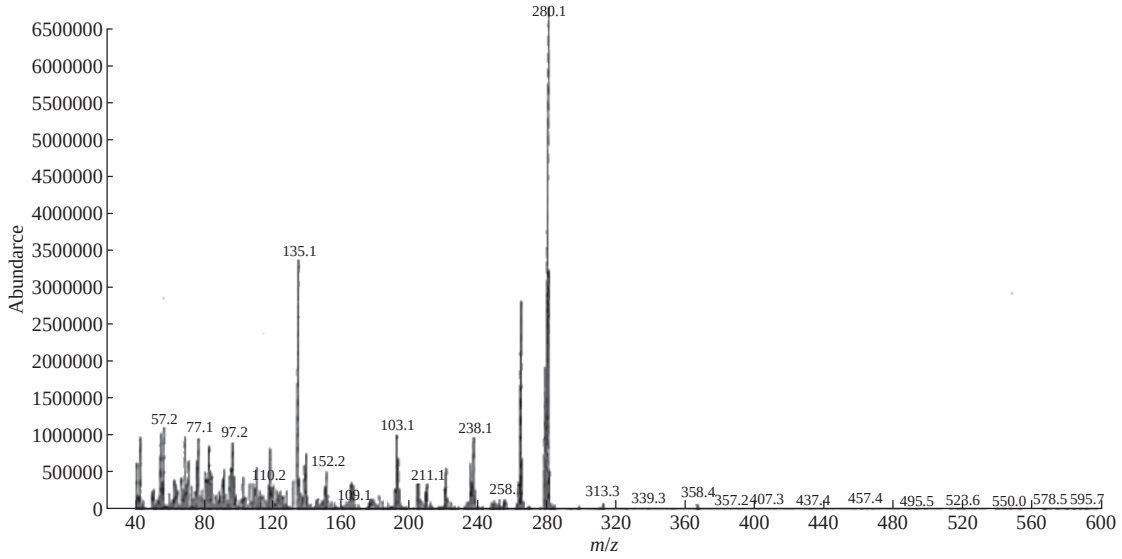

Fig. 1 Mass spectra of azo ligand (AAMPI).

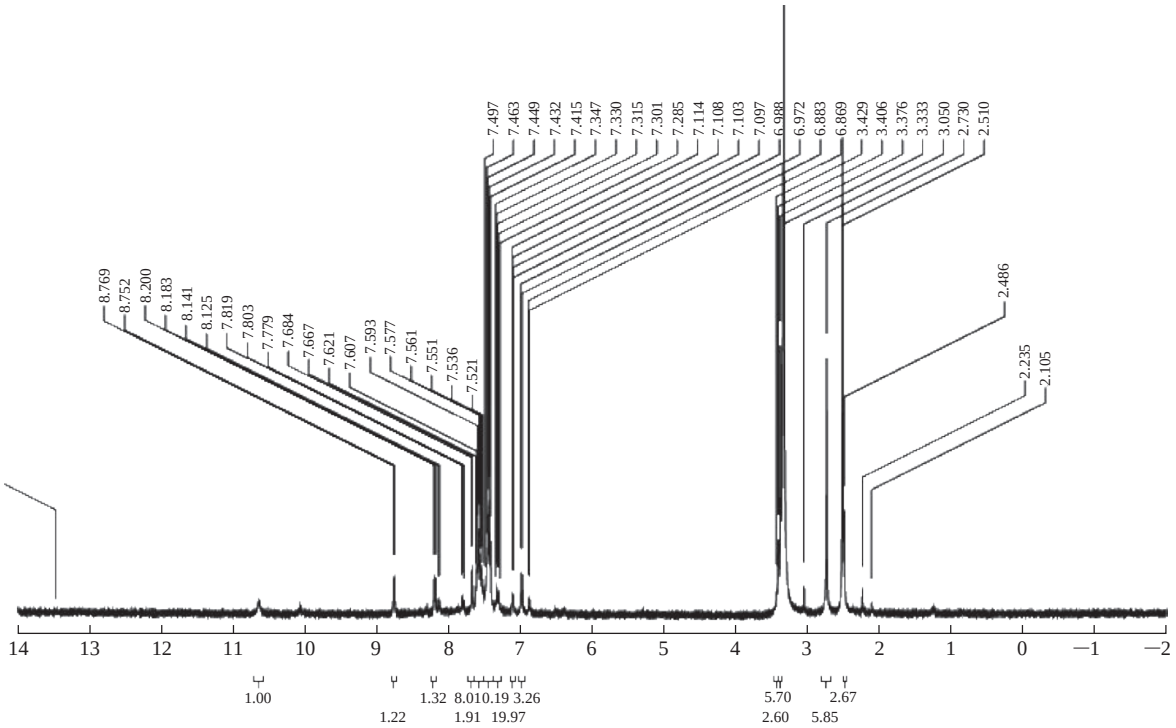

Fig. 2 HNMR Spectra of azo ligand (AAMPI).

Carbon-13 nuclear magnetic resonance (^{13}CNMR) spectra

The ^{13}CNMR of the azo ligand showed several signals in Fig. 3. The signal observed at 158 ppm was attributed to the carbonyl group of amide C=O in antipyrine. The peak at 34 ppm was attributed to the methyl group N-CH_3 of antipyrine ring, while the signal at 155 ppm was attributed to C3 of pyrazole ring. The signals at 135, 127, 129 and 130 ppm referred to C1, C2, C3 and C4 of phenyl of the antipyrine ring, respectively. The imidazole derivative gave a signal at 56 ppm to the 2- methoxy group, a signal at 126 ppm to C4 and C5 of imidazole rang, while a signal at 153 ppm to C2, and the signals at 134, 128, 114 and 156 to C1, C2, C3 and C4 of imidazole phenyl ring, respectively.

FT-IR Spectra

The IR spectra explain valuable information related to the nature of functional group attached to the metal atom. In order to study the binding method of the ligand to metal ion in the complexes, the IR spectrum of the free ligand (AAMPI) was compared with the symmetric metal ion complexes. The chosen vibrational bands of the ligand with metal complexes are listed in Table 2. The IR spectra of the ligand and Co (II) complex are explicit in Fig. 4 and 5. The IR spectrum of the ligand showed a medium and broad band around 3433/cm, which can be referred to υ(N-H) stretching vibration of derivative imidazole. The spectrum of ligand showed a band at 1475/cm due to the N=N group. Thus the band appearing at 1462-1485/cm in all spectra of metal complexes shifted to a lower wave number with differences in shape and reduced in intensity of the spectra of complexes. The band shifted and reduced intensity due to the complex formation [21]. Strong band at 1643/cm in the ligand was observed due to υ(C=O) of the Kato group in a pyrazolone ring [22] in the complexes. The band shifted to lower frequency at 1616-1654/cm, indicating the coordination of carbonyl oxygen to the metal ion.

The spectrum of free ligand showed the absorption band at 154/cm due to υ(C=N) of the N3 derivative imidazole nitrogen. In the complexes, this band shifted

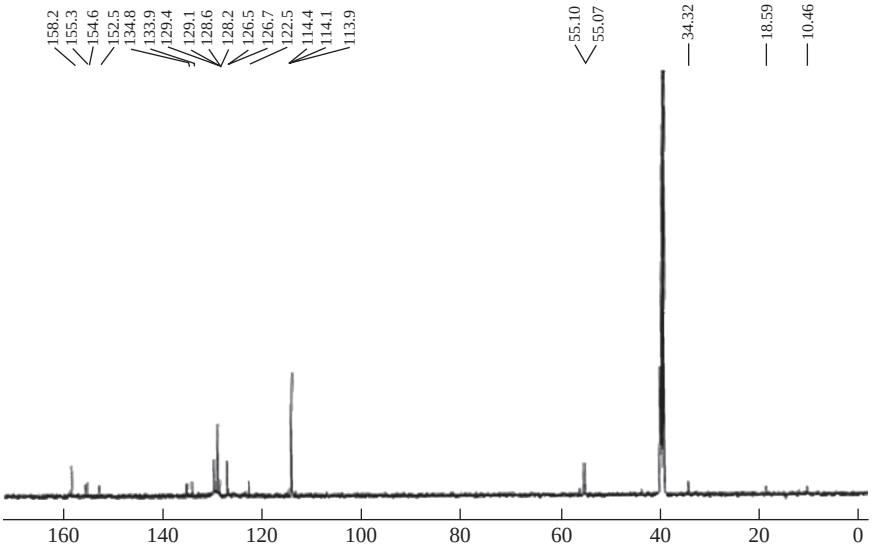

Fig. 3 CNMR Spectra of azo ligand (AAMPI).

Table 2 Characteristic IR absorption bands of the ligand and its complexes

Compounds	ν(N-H)	ν(C-H)or	ν(C-H)al	ν(C=O)	ν(C=N)	ν(N=N)	ν(M-O)	ν(M-N)
AAMPI	3433m	3010w	2949w	1643s	1548s	1475m	-	-
$[Co(AAMPI)_2]Cl_2{\cdot}H_2O$	3408w	3003w	2962w	1633m	1519m	1465w	534w	459w
$[Ni(AAMPI)_2]Cl_2{\cdot}H_2O$	3414m	3003w	2937w	1620s	1517s	1463w	505w	424w
$[Cu(AAMPI)_2]Cl_2{\cdot}H_2O$	3425w	3005w	2901w	1616m	1525s	1462w	532w	470w
$[Zn(AAMPI)_2]Cl_2{\cdot}H_2O$	3448w	3006w	2931w	1651m	1516m	1462w	528w	439w
$[Cd(AAMPI)_2]Cl_2{\cdot}H_2O$	3429m	3171w	2935w	1647m	1516m	1485w	532w	443w
$[Hg(AAMPI)_2]Cl_2{\cdot}H_2O$	3410w	3015w	2935w	1654m	1520m	1462w	532w	460w

Note: s = strong; m = medium; w = week.

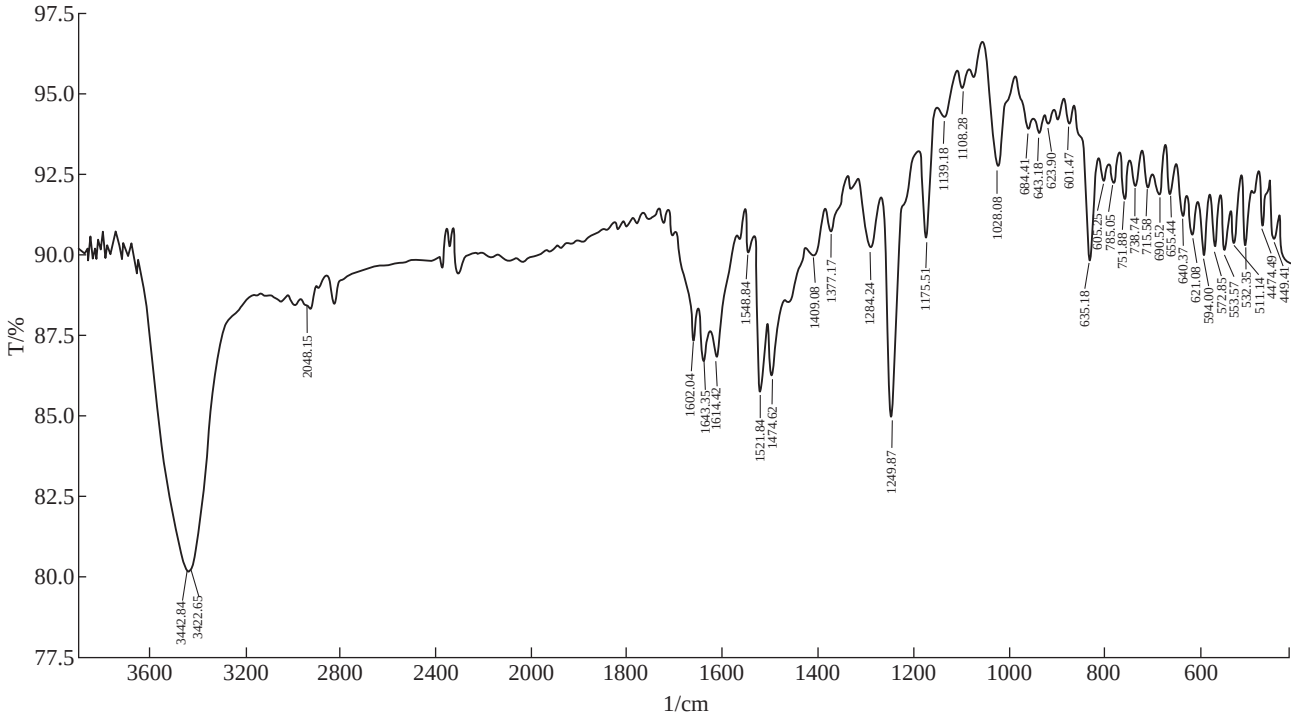

Fig. 4 FT-IR spectra of azo ligand (AAMPI).

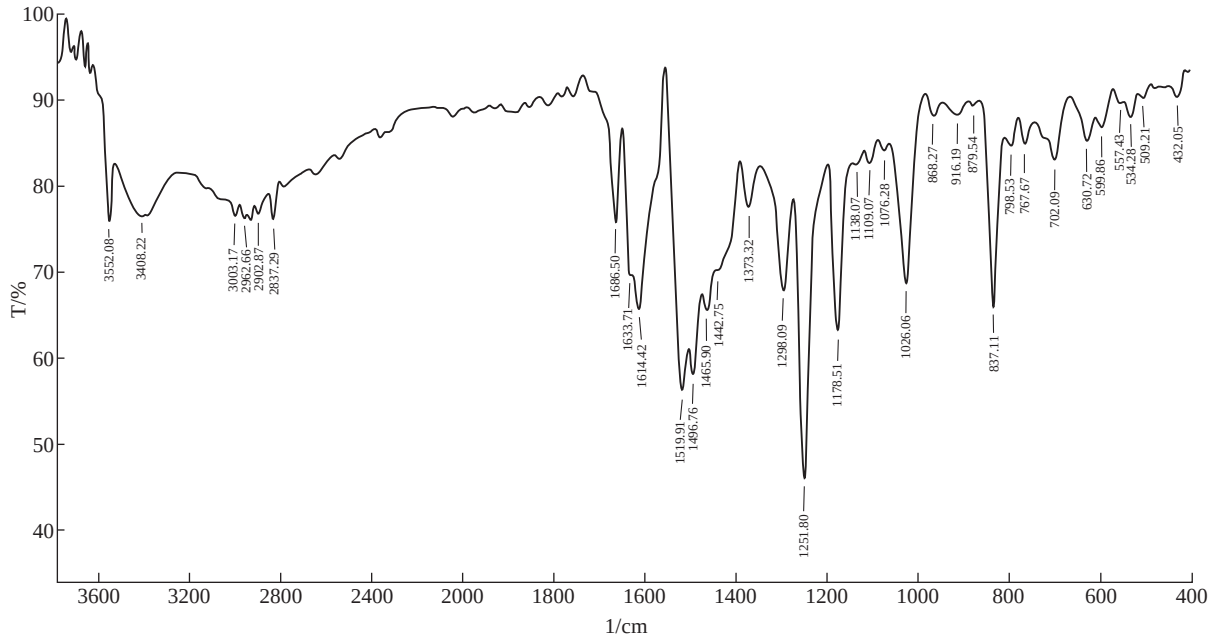

Fig. 5 FT-IR spectra of Co (II) complex.

to a lower frequency at 1516-1525/cm [23], which was further supported by the formation of new bands in the range of 534-505/cm attributed to υ(M-O) and bands 460-424/cm attributed to υ(M-N) [24]. The complexes showed a broad band at 3448-3410/cm, suggesting a coordination of water with metal complexes [25]. Thus, the above IR spectral information led to indicating that the ligand behaved as a neutral tridentate chelating, and the coordination sites were the N3 atom of the hetero cyclic imidazole ring, nitrogen atom of azo group nearest to a phenyl ring, and a carbonyl group of pyrazolone ring, to give two quinapril chelate ring.

Electronic spectra

Electronic spectra of the metal complexes were recorded in the UV-Vis region of 200-1100 nm in ethanol solution. The spectral data and the magnetic moment of prepared complexes are shown in Table

3. UV-Vis spectral studies of the metal complexes exhibited a transition at lower than 500 nm, corresponding to intramolecular n→π* and π→π* charge-transfer transitions [26]. Intense absorption bands (ε~10^4) appeared in the range of 458-493 nm for the complexes, which might be attributed to the d M→π* (ligand) charge-transfer transition [27]. The electronic spectra of the ligand and the Co (II) are shown in Fig. 6 and 7.

Molar conductivity

Molar conductance of the metal complexes was measured in DMSO as a solvent at room temperature.

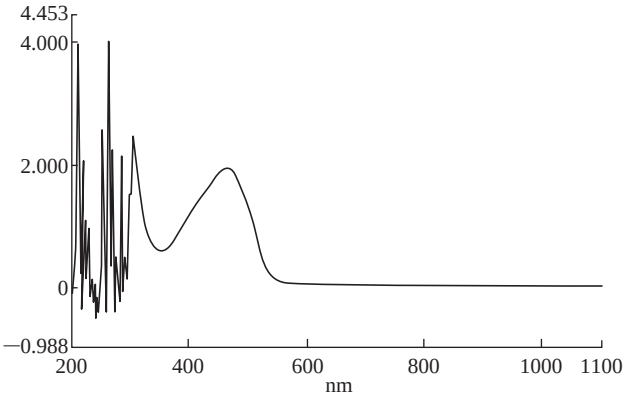

Fig. 6 UV-Vis spectra of azo ligand (AAMPI).

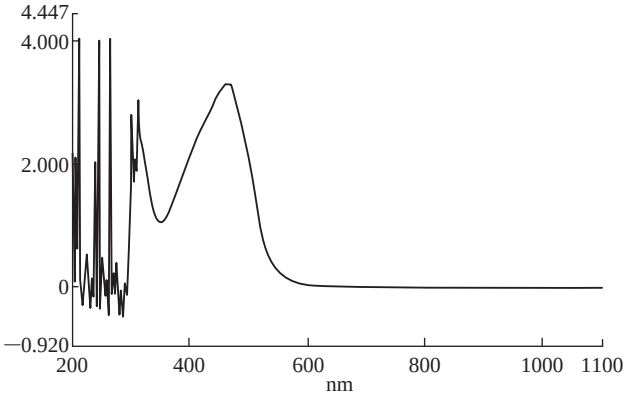

Fig. 7 UV-Vis spectra of Co (II) complexes.

The high values of molar conductivity for the complexes referred to the electrolytic nature of M : L ratio which was 1:2 due to chloride ion Cl^- outside the coordination sphere, as shown in Table 3.

Magnetic measurements

The magnetic moment values for metal complexes (Fig 3) have been used as a criterion to define the type of coordination for the metal ion, on account of the intrinsic orbital angular momentum in the round state. In the metal complexes, the magnetic moment of 4.90 B.M. suggested an octahedral geometry for the Co(II) complex in the high spin state; magnetic moment value of 3.06 B.M. for a high-spin Ni(II) complex depended on the magnitude of the orbital contribution. For Cu(II) complex, the magnetic moment value of 1.77 B.M. was expected for one unpaired electron which offered the potential of an octahedral geometry. And the magnetic moment values of Zn(II), Cd(II) and Hg(II) metal complexes were diamagnetic and consistent with the d^{10} configuration [28]. Depending on these results, the structure of the chelate complexes was proposed in Fig. 8.

Antimicrobial activity

All the newly synthesized compounds were screened for their antibacterial and antifungal activities. The data of antibacterial activity of the prepared free ligand (AAMPI) and its metal complexes were summarized in Table 4; its statistical presentation is shown in Fig. 1. The effect of the free ligand and its chelate complexes were tested in vitro against *P. mirabillis*, *K. pneumoniae*, *P .aeruginosa*, *S. epidermidis* and *S. aureus*. It is clear that the inhibition by metal complexes was higher than that of free ligand. The ligand showed moderate effect against tested bacterial strains. The Cd (II) and Hg (II) complexes exhibited high activity against all bacteria. The Cu (II) and Zn (II) complexes had high potency as antibacterial for

Table 3 Spectral data, conductivities, magnetic moment and proposed structure of prepared complexes

Complex	Assigument	Absorption band (nm)	LM (S·cm^2/mol)	μ_{eff} (B.M)	Proposed structure
AAMPI	n→p* & π→p*	440,312,245	-	-	-
$[Co(AAMPI)_2]Cl_2{\cdot}H_2O$	C. T.	464	70.12	4.90	Oh
$[Ni(AAMPI)_2]Cl_2{\cdot}H_2O$	C. T.	463	86.32	3.06	Oh
$[Cu(AAMPI)_2]Cl_2{\cdot}H_2O$	C. T.	473	75.60	1.77	Oh
$[Zn(AAMPI)_2]Cl_2{\cdot}H_2O$	C. T.	459	71.2	Dia	Oh
$[Cd(AAMPI)_2]Cl_2{\cdot}H_2O$	C. T.	458	79.6	Dia	Oh
$[Hg(AAMPI)_2]Cl_2{\cdot}H_2O$	C. T.	493	80.4	Dia	Oh

Note: S = Surface of medium

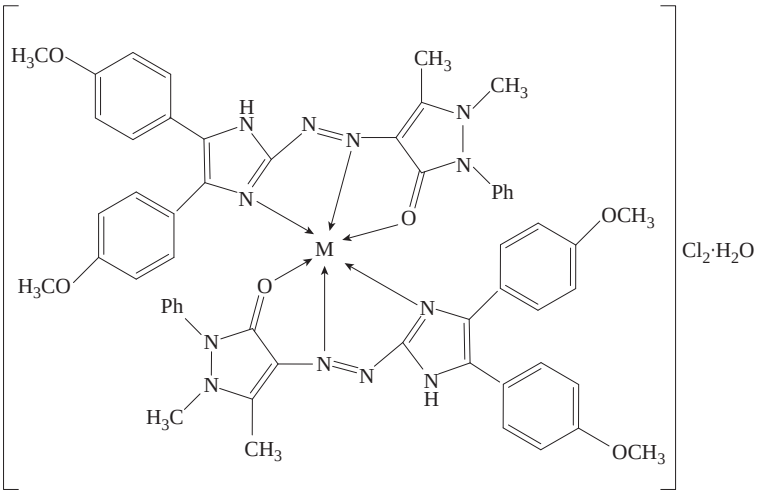

M=Co(II), Ni(II), Cu(II), Zn(II), Cd(II) and Hg

Fig. 8 The proposed structural formula of the metal chelate complex.

Table 4 Antibacterial activity data (zone of inhibition in mm) of the ligand and their metal complexes

Compound	Bacteria				
	Gram-negative (G) -ve			Gram-positive (G) +ve	
	P. mirabillis	*K. pneumonia*	*P. aeruginosa*	*S. epidermidis*	*S. aureus*
(L)=AAMPI	11	10	10	10	9
$[Co(L)_2]Cl_2·H_2O$	13	12	11	11	11
$[Ni(L)_2]Cl_2·H_2O$	12	12	13	13	13
$[Cu(L)_2]Cl_2·H_2O$	13	13	13	14	12
$[Zn(L)_2]Cl_2·H_2O$	14	14	16	13	11
$[Cd(L)_2]Cl_2·H_2O$	15	16	15	15	14
$[Hg(L)_2]Cl_2·H_2O$	16	14	17	15	15

Note: High activity = Inhibition Zone > 12 mm and moderate = Inhibition Zone = A – 12mm.

all bacteria except *S. aureus* for which a moderated potency was shown. The Co (II) complex had moderate effect against most tested bacteria except *P. mirabillis* for which a high effect was shown. The Ni (II) showed high potency against gram-positive bacteria and *P. aeruginosa*, with the exception of *P. mirabillis* and *K. pneumoniae* for which a moderate effect was shown. The ligand and its chelate complexes exhibited high to moderate activity against the same bacteria strains. Also, it was observed that the compounds were more active against gram-negative than against gram-positive bacteria.

Concerning in vitro fungicidal activity, the data in Table 5 reveal that all the metal complexes had high activity than the free ligand. A comparative study of the newly prepared compounds indicated a high antifungal activity in comparison to the free ligand. Substantial activity was achieved in case of Hg(II) complex against most bacteria and fungi. However, the compounds appeared significantly toxic at 1000 ppm conc., against all species of fungi. In addition, all chelate complexes were more active than the free ligand, and antifungal potency decreased upon dilution. When the comparison for the compounds was made between bacteria and fungi, the compounds were found to be more active against fungi than against bacteria. This would suggest that the chelation of the complex easily crossed a cell membrane [29]. The change in effectiveness of different biocidal species against microbial depended on impermeability of the cell of microbes or on differences in ribosome of microbial cells [29, 30]. The highest activity of the complexes may be attributed to the different properties of metal ions upon chelation, in which the metal ion was adsorbed on the cell wall of the microbial. The metal ions are essential for the growth inhibitory influence [31-34]. They increase lipophilicity, enhance the penetration of the complexes into lipid membranes and the blocking of the metal binding sites in the enzymes of microorganisms. Due to the presence of more functional groups such as the >C=N-azomethine group, which forms hydrogen bonds with active centers of cell constituents of the microbial,

Table 5 Average percentage fungi inhibition after 72 h (%)

Compound Conc.:	Fungi								
	A. niger			*F. oxysorium*			*T. horzianum*		
	250	500	1000	250	500	1000	250	500	1000
L = AAMPI	65.65	68.89	74.44	66.67	67.78	71.11	54.44	65.56	65.56
$[Co(L)_2]Cl_2{\cdot}H_2O$	71.11	71.11	81.11	73.33	75.56	83.33	67.78	71.11	77.78
$[Ni(L)_2]Cl_2{\cdot}H_2O$	75.56	80	87.78	70	72.22	76.67	61.11	66.67	73.33
$[Cu(L)_2]Cl_2{\cdot}H_2O$	81.11	84.44	90	78.89	82.22	92.22	71.11	75.56	81.11
$[Zn(L)_2]Cl_2{\cdot}H_2O$	68.89	76.67	82.22	77.78	85.56	88.89	68.89	72.22	77.78
$[Cd(L)_2]Cl_2{\cdot}H_2O$	86.67	93.33	95.56	85.56	87.78	94.44	72.22	74.44	80
$[Hg(L)_2]Cl_2{\cdot}H_2O$	83.33	88.89	96.67	80	86.67	91.11	78.89	85.56	88.89

Note: Conc. in ppm

resulting in interference with the normal cell process [34, 35]. The mechanism of active antimicrobial agents can be discussed under five headings; inhibition of cell wall synthesis, alteration of cell membrane function, inhibition of nucleic acids synthesis, inhibition of protein synthesis and inhibition of metabolic pathways [29, 35, 36].

Conclusions

According to above results, a significant biological activity against microorganisms was observed for the synthesized metal complexes compared to free ligand. It was also noticed that the ligand behaved in natural tridentate manner in the coordination with metal ions. All the complexes exhibited octahedral geometry around the metal center. The complexes were stable and not ionic.

Conflict of Interests

The authors declare that no competing interest exists.

References

[1] M. Sheikhi, S. Shahab, and L. Filippovich, New derivatives of (E, E)-azomethines: Design, quantum chemical modeling, spectroscopic (FT-IR, UV/Vis, polarization) studies, synthesis and their applications: Experimental and theoretical investigations. *Journal of Molecular Structure*, 2018, 1152: 368-385.

[2] H. Chen, J. Motuzas, J.C. Diniz da Costa, et al., Degradation of azo dye Orange II under dark ambient conditions by calcium strontium copper perovskite. *Applied Catalysis B: Environmental*, 2018, 221: 691-700.

[3] A. Gilewska, J. Masternak, K. Kazimierczuk, et al., Synthesis, structure, DNA binding and anticancer activity of mixed ligand ruthenium (II) complex. *Journal of Molecular Structure*, 2018, 1155: 288-296.

[4] S.S. Kumar, S. Biju, and V. Sadasivan, Synthesis, structure characterization and biological studies on a new aromatic hydrazone, 5-(2-(1,5-dimethyl-3-oxo-2-phenyl-2,3-dihydro-1H-pyrazol-4-yl) hydrazono)-2, 2-dimethyl-1, 3-dioxane-4, 6-dione, and its transition metal complexes. *Journal of Molecular Structure*, 2018, 1156: 201-209.

[5] H. Tabor, Metabolic studies on histidine, histamine, and related midazoles. *Pharmacological Reviews*, 1954, 6(3): 299-343.

[6] R. Kenchappa, Y.D. Bodke, and S. Telkar, Antifungal and anthelmintic activity of novel benzofuran derivatives containing thiazolo benzimidazole nucleus: An in vitro evaluation. *Journal of Chemical Biology*, 2017, 10(1): 11-23.

[7] M.V. Papadopoulou, W.D. Bloomer, and H.S. Rosenzweig, The antitubercular activity of various nitro (triazole/imidazole)-based compounds. *Bioorganic & Medicinal Chemistry*, 2017, 25(21): 6039-6048.

[8] R.T. Iminov, A.V. Tverdokhlebov, A.A. Tolmachev, et al., Simple and convenient synthesis of 2, 3, 4, 5-tetrahydro-1, 5-dioxopyrrolo [1, 2-a] quinazoline-3a (1H)-carboxylic acids in multi-gram scale. *Heterocycles*, 2008, 75(7): 1673-1680.

[9] N. Liu, D. Ding, L. Wang, et al., Two novel Mg(II)-based and Zn (II)-based complexes: inhibiting growth of human liver cancer cells. *Brazilian Journal of Medical and Biological Research*, 2018, 51(2).

[10] K. Karrouchi, S. Radi, and Y. Ramli, Synthesis and Pharmacological Activities of Pyrazole Derivatives: A Review. *Molecules*, 2018, 23(1): 134.

[11] P. Palanisamy, S.J. Jenniefer, and P.T. Muthiah, Synthesis, characterization, antimicrobial, anticancer, and antituberculosis activity of some new pyrazole, isoxazole, pyrimidine and benzodiazepine derivatives containing thiochromeno and benzothiepino moieties. *RSC Advances*, 2013, 3(42): 19300-19310.

[12] M.A. Metwally, Y.A. Suleiman, M.A. Gouda, et al., Synthesis, antitumor and antioxidant evaluation of some new antipyrine based azo dyes incorporating pyrazolone moiety. *Int. J. Mod. Org. Chem*, 2012, 1(3): 213-225.

[13] J.R.E. Hoover, A.R. Day, Preparation of some imidazole derivatives of 1, 4-naphthoquinone. *Journal of the American Chemical Society*, 1954, 76(16): 4148-4152.

[14] S. Shibata, M. Furukawa, and R. Nakashima,Syntheses of azo dyes containing 4, 5-diphenylimidazole and their evaluation as analytical reagents. *Analytica Chimica Acta*, 1976, 81(1): 131-141.

[15] H. Huheey, E.A. Keiter, and R.L. Keiter, *Inorganic chemistry: principles of structure and reactivity*, 4th ed. Harper Collin College Publishers, 1993.

[16] N. Raman., J.D. Raja, Synthesis, structural,

characterization and antibacterial studies of some bio sensitive mixed ligand copper (II) complexes. *Indian J. Chem.*, 2007, 46A: 1611-1614.

[17] A.S. Al-Rammahi, A.H. Al-khafagy, and F.A. Al-Rammahi, Synthesis and characterization of oxazepen and imidazolin derivatives from 2-amino -5- mercapto 1,3,4-thiadiazol and studing of their biological activity. *World J. pharm. Res.*, 2015, 4(2): 1668-1680.

[18] A.H. Al-Khafagy, Synthesis, characterization and biological study of some new metal-azo chelate complexes. *J. Chem. Pharm. Res.*, 2016, 8(8): 296-302.

[19] A. Saeyda, Synthesis and characterization of some metal complexes derived from azo compound of 4, 4′-methylenedianiline and antipyrine: evaluation of their biological activity on some land snail species. *Journal of Molecular Structure*, 2015, 1099: 567-578.

[20] S. Suhad, Synthesis and spectral studies of heterocyclic azo dye complexes with Y (III) and La (III) ions. *Al-Qadisiyah Journal of Pure Science*, 2017, 19(1): 67-77.

[21] T. Giuseppe, Ligating properties of thionitrosoamines: I. neutral mononuclear N-thionitrosodimethylamine-palladium (II) and-platinum (II) complexes. *Journal of Organometallic Chemistry*, 1983, 252(3): 381-387.

[22] C. Gyana, Cobalt (II) complexes of ONO donor Schiff bases and N, N donor ligands: synthesis, characterization, antimicrobial and DNA binding study. *International Journal of Research in Chemistry and Environment*, 2013, 32: 172-180.

[23] P.A.L. Sanjib, Synthesis, spectral and electrochemical properties of 1-alkyl-2-(naphthyl-β-azo) imidazole complexes of platinum (II) and the reaction with pyridine bases. Single-crystal X-ray structure of dichloro-[1-ethyl-2-(naphthyl-β-azo) imidazole] platinum (II). *Polyhedron*, 2000, 19(10): 1263-1270.

[24] S. Ayşe, Studies on mononuclear transition metal chelates derived from a novel (E, E)-dioxime: synthesis, characterization and biological activity. *Journal of Coordination Chemistry*, 2007, 60(6): 655-665.

[25] K. Nakamoto, *Infrared and Raman spectra of inorganic and coordination compounds*, 6rd ed. A John Wiley & Sons, Inc., 2009: 1-29, 57-62, 67, 313.

[26] G. Valarmathy, R. Subbalakshmi, Synthesis, spectral characterization of biologically active novel Schiff base complexes derived from 2-sulphanilamidopyrimidine. *Int. J Pharma Bio Sci*, 2013, 4(2): 1019-1029.

[27] S. Pal, C. Sinha, Studies on the reactivity of cis-$RuCl_2$ fragment in Ru (PPh3)2 (TaiMe) Cl_2 with N, N-chelators (TaiMe= 1-methyl-2-(p-tolylazo) imidazole). Spectral and electrochemical characterisation of the products. *Journal of Chemical Sciences*, 2001, 113(3): 173-183.

[28] R.A. Oatto, S. Yamal, *An elements of magnetic chemistry*, 2nd ed. East West press, 1993: 101.

[29] S. Subramanian, N. Rammaswamy, and B. Kartha, Synthesis of mononuclear Schiff base Cu(II), Ni(II), Co(II) and Mn(II) complexes and their application for DNA cleavage and antibacterial agent. *Chem. Sci. Rev. Lett.*, 2015, 14(13): 121-128.

[30] S.S Mary, S. Shobana, and J. Dharmaraja, In vitro microbial and antioxidant activities of Mn(II) mixed ligand complexes. *J. Chem. Pharm. Res.*, 2016, 8(1S): 12-18.

[31] R.S. Joseyphs, M.S. Nair, Antibacterial and antifungal studies on some Schiff base complexes of Zn(II). *Mycobiology*, 2008, 36(2): 93-98.

[32] N. Raman, D.J. Raja, and A. Sakthivel, Synthesis, spectral characterization of Sciff base transition metal complexes; DNA cleavage and antimicrobial activity studies. *J. Chem. Sci.*, 2007, 119(4): 303-309.

[33] A.A. Algon, S.S. Chyad, perilipin-1 level as risk marker of insulin resistance in morbidly obese patients. *Nano Biomed. Eng.*, 2017, 9(4): 285-290.

[34] R.S. Al-Zabeba, E. Grulke, Interaction of calcium phosphate nanoparticles with human chorionic gonadotropin modifies secondary and tertiary protein structure. *Nova Biotechnologica et Chimica*, 2015, 14(2): 141-157.

[35] R.K. Al-Shemary, B.A. Zaidan, Preparation and characterization of some transition metal complexes of new tetradentate Schiff base ligand type N_2O_2. *Sch. Acad. J. BioSci.*, 2016, 4(1): 18-26.

[36] N. Salih, J. Salimon, and E. Yousif, Synthesis, characterization and antimicrobial activity some carbamothioyl 1,3,4-thiadiazole derivatives. *International J. Pharm. Tech. Res.*, 2012, 4(2): 655-660.